

Anti-Oxidative Passivation and Electrochemical Activation of Black Phosphorus via Covalent Functionalization and Its Nonvolatile Memory Application

Weilin Chen,^{a,b} Shuang Gao,^{*a} Zhuolin Xie,^{a,b} Ying Lu,^{a,b} Guodong Gong,^{a,b} Gang Liu,^{*c} Jie Shang,^a Chuang Yao,^d and Run-Wei Li^{*a}

^aCAS Key Laboratory of Magnetic Materials and Devices, and Zhejiang Province Key Laboratory of Magnetic Materials and Application Technology, Ningbo Institute of Materials Technology and Engineering, Chinese Academy of Sciences, Ningbo 315201, China.

Email: gaoshuang@nimte.ac.cn, runweili@nimte.ac.cn

^bCollege of Materials Sciences and Opto-Electronic Technology, University of Chinese Academy of Sciences, Beijing 100049, China.

^cSchool of Electronic Information and Electrical Engineering, Shanghai Jiao Tong University, Shanghai 200240, China. Email: gang.liu@sjtu.edu.cn

^dKey Laboratory of Extraordinary Bond Engineering and Advance Materials Technology (EBEAM) of Chongqing, School of Materials Science and Engineering, Yangtze Normal University, Chongqing 408100, China.

Part 1: Experimental Section

Synthesis of DTPA: The DTPA was synthesized *via* diazotation reaction according to ref. [1]. To be specific, 1.84 g of 4-Aminotriphenylamine (ATPA) together with 48% HBF₄ (20 mL, 154 mmol) and 10 mL of water was firstly placed in a 100 mL round bottom flask equipped with a stir bar. The flask was then cooled to 0 °C in an ice bath. Next, a solution of NaNO₂ (2 g, 29 mmol) in 20 mL of water was cooled to 0 °C and added dropwise into the flask with stirring. A small amount of gas evolution was observed during the addition process. After that, the flask was covered with aluminum foil to exclude light and stirred for 5 hours as it slowly warmed to room temperature. Subsequently, an additional solution of NaNO₂ (1g) in 5 mL of water was cooled to 0 °C and slowly added to the reaction mixture, again with some gas evolution. The obtained mixture was again cooled to 0 °C in an ice bath, followed by the addition of a second portion of NaNO₂ (1 g) in 5 mL of water. Then the mixture was allowed to warm to room temperature and stirred for 20 hours until none of the starting material remained. Suspended in the orange solution right now were clay-colored precipitates. Finally, the mixture was cooled to 0 °C and filtered by suction with ice-cold 4% HBF₄ to give clay-brown precipitates.

Preparation of BPNSs: BP crystals were purchased from Smart Elements and stored in a dark Ar-filled glove box. About 200 mg of BP crystals were firstly ground to power in a glove box and then dispersed in 50 mL degassed N-methyl pyrrolidinone (NMP). Next, a custom setup of tip sonicator was used to exfoliate BPNSs for 10 h in an ice bath. The resultant dispersion was then centrifuged at 5000 rpm for 30 min, leading to the supernatant containing BPNSs. Finally, the supernatant was centrifuged at high speed of 11000 rpm for 30 minutes to give precipitation of BPNSs, which was washed with degassed acetonitrile for several times to remove the residual NMP.

Synthesis of BPNSs-TPA: The BPNSs-TPA was deliberately synthesized *via* the spontaneous reaction between aryl diazonium salts and BPNSs under aqueous conditions. In a typical reaction, a mixture of DTPA (360 mg, 1 mol) and tetrabutylammonium hexafluorophosphate (387 mg, 1 mol) in acetonitrile (50 mL) was added dropwise to the stirred BPNSs (100 mg) dispersion in acetonitrile by magnetic stirring under argon protection for 5 hours. After the reaction, the obtained dispersion was centrifuged at 11000 rpm for 30 min to remove the solvent. The obtained precipitate was then washed with degassed acetonitrile for several times to remove residual tetrabutylammonium hexafluorophosphate

and excessive DTPA and then dried under vacuum overnight to give BPNSs-TPA.

Characterization of the synthesized materials

FTIR spectra were recorded using Spectrum 100 spectrophotometer (Nicolet 6700, Thermo). ^1H NMR analysis was conducted on AVANCE III 400MHz (Bruker). Atomic force microscopy (AFM) measurements were performed on an ICON Bruker system in tapping mode at a scan rate of 1 Hz. TEM and EDS images were obtained by a transmission electron microscope (Talos F200x, FEI). Raman measurements were carried out using a Raman microscopic system equipped with 532 nm excitation laser beam (inVia Reflex, Renishaw). XPS measurements were performed on an Axis Ultra DLD spectrometer (Kratos). UV-vis absorption spectra was recorded on a UV-vis spectrometer (Lambda 950, Perkin-Elmer). Cyclic voltammetry (CV) measurements were conducted on a model CHI 650D electrochemical workstation (Modulab).

Theoretical calculations

The geometric structures and formation energies were calculated using DFT with the Perdew-Burke-Ernzerhof (PBE) energy functional and a plane-wave pseudopotential formalism. The calculations were performed including gradient corrections *via* the generalized gradient approximation (GGA) with the CASTEP computer code in materials studio.

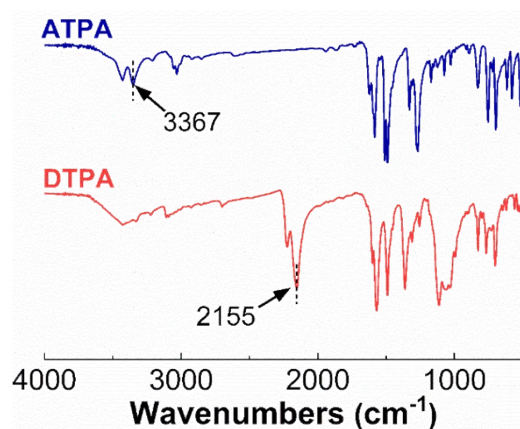
Device Fabrication and Characterization

The BPNSs-TPA@PVP solution of 0.2 mg/mL was prepared by re-dispersing the prepared BPNSs-TPA in polyvinylpyrrolidone (PVP, Mw ~50000) solution in ethanol (20 mg/mL), while the $\text{EV}(\text{ClO}_4)_2$ @PEO solution was obtained based on previous report in ref. [2]. Before device fabrication, the indium-tin oxide (ITO) substrate was firstly cleaned by acetone, ethanol, and deionized water in sequence and then treated with O_2 plasma. Then, a layer of BPNSs-TPA@PVP was spin-coated onto the substrate at 4000 rpm for 30 s, followed by dried under vacuum for 2 hours. Similarly, the $\text{EV}(\text{ClO}_4)_2$ @PEO layer was spin-coated at 2000 rpm for 60 s and dried under vacuum for 2 hours. The thicknesses of BPNSs-TPA@PVP and $\text{EV}(\text{ClO}_4)_2$ @PEO layers were estimated to be ~105 and ~185 nm, respectively, by the use of a scanning electron microscope (SEM, Verios G4 UC, Thermo) (Figure S12, Supporting Information). Finally, circular top electrodes with a diameter of 150 μm and consisting of 10 nm Ti and 80 nm Pt were deposited by E-beam evaporation through a metal shadow mask at room temperature. All electrical measurements were performed using a

semiconductor device analyzer (B1500A, Agilent) in ambient conditions without any device encapsulation.

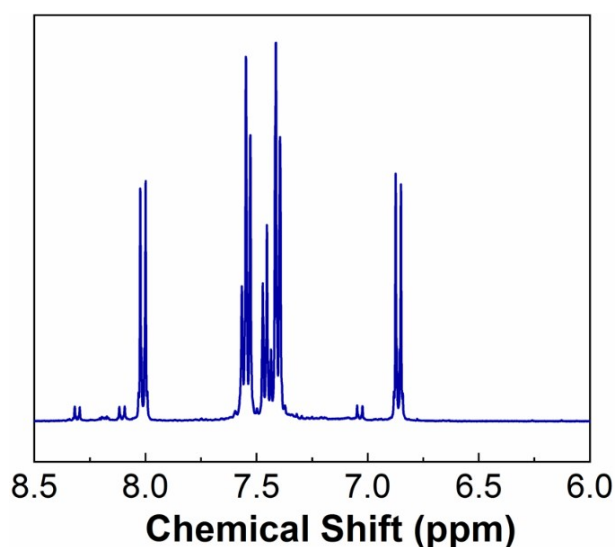
Part 2: Supporting Figures

Figure S1. FTIR spectra of the ATPA and DTPA.



As shown in **Figure S1**, the characteristic vibrational peak at 3367 cm⁻¹ corresponds to amino-group (-NH₂). After diazotization, amino-group (-NH₂) characteristic vibrational peak disappeared in the FTIR spectrum of DTPA, followed by the appearance of characteristic vibrational peak of diazo group (-N₂⁺) at 2155 cm⁻¹.

Figure S2. ¹H NMR spectrum of DTPA.



As shown in **Figure S2**, ¹H NMR (400MHz, CD₃CN, ppm) of the prepared DTPA: 8.00 (d, 2H), 7.55 (m, 4H), 7.48-7.37 (m, 6H), 6.86 (d, 2H).

Figure S3. AFM image of BPNSs in a large area.

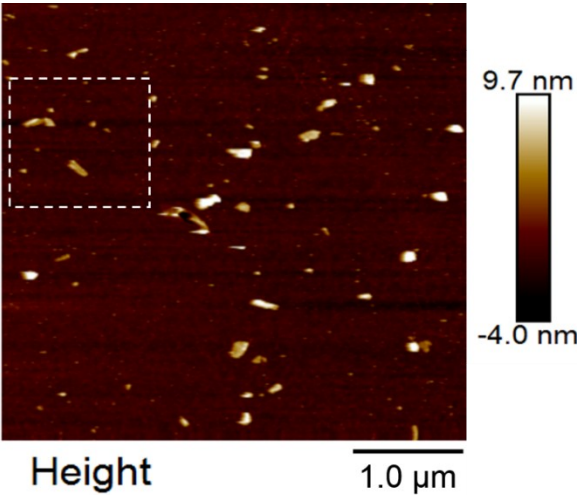


Figure S4. AFM characterization of BPNSs. a) Magnified AFM image taken from a selective area in Figure S3. b) Height profiles along the white lines in a). c-d) Statistical analysis of heights and lengths of BPNSs measured by AFM.

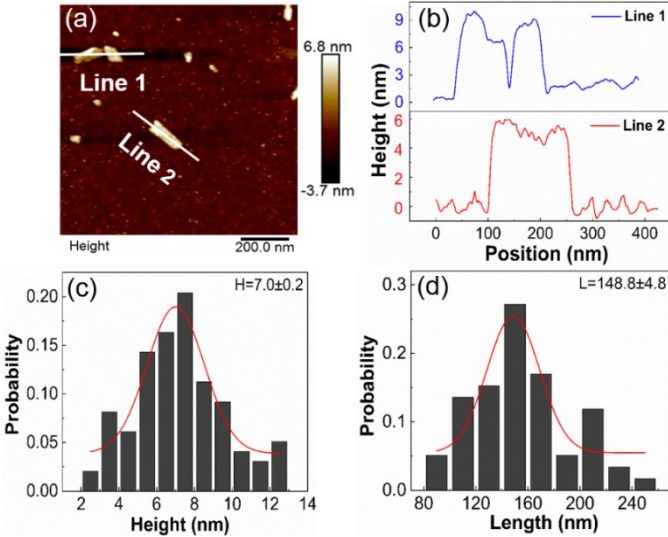


Figure S5. TEM image and EDS maps of BPNSs.

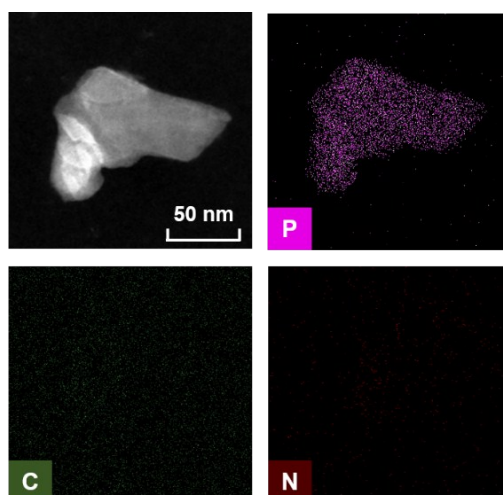


Figure S6. Raman analysis of BPNSs-TPA. a) Scanning Raman microscopy mapping of BPNSs-TPA based on the A^1_g/A^2_g intensity ratio. b) Typical Raman spectra of the areas marked in a).

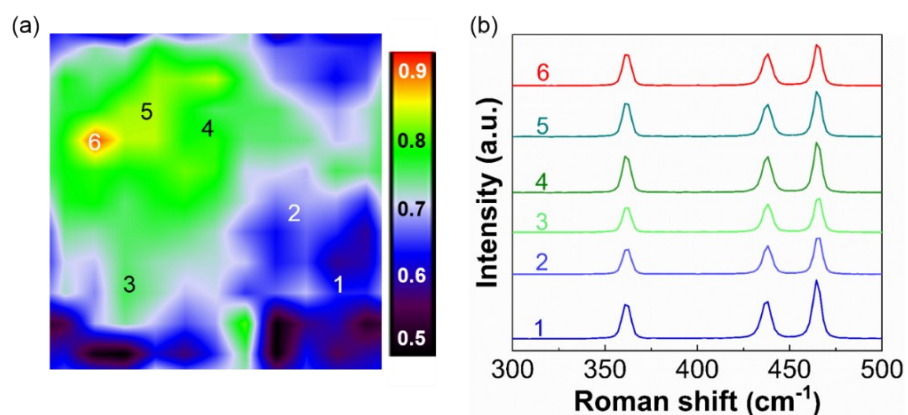


Figure S7. Comparison of degradation rates of different protection strategies reported in the literature.

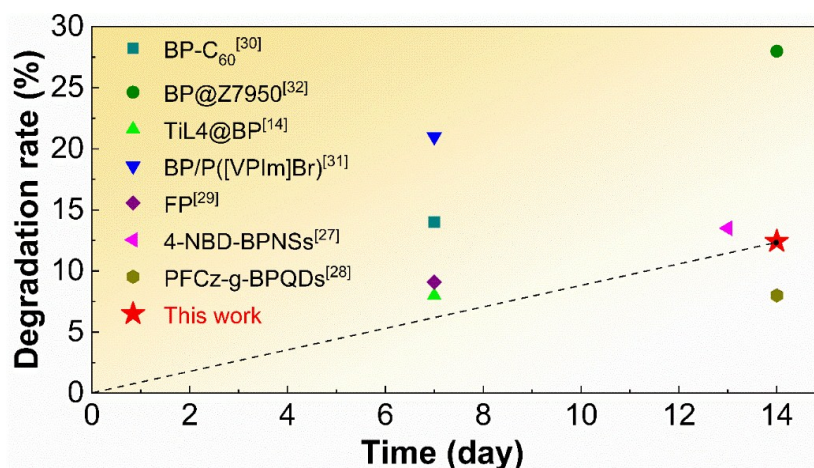


Figure S8. Magnified CV plots of the a) BPNSs and b) BPNSs-TPA samples.

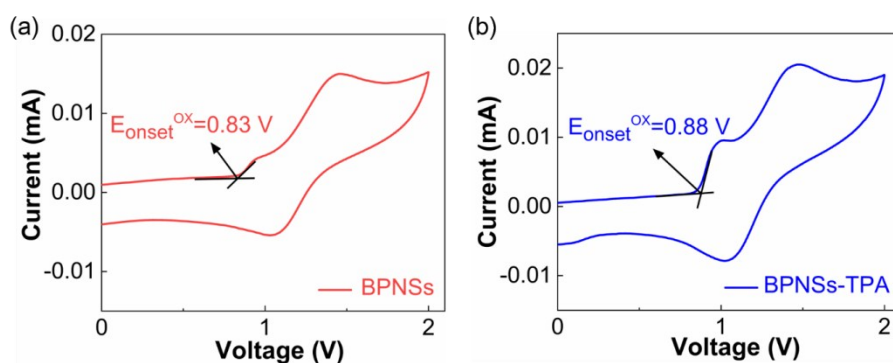


Figure S9. Consecutive voltage stimulations of the $\text{EV}(\text{ClO}_4)_2/\text{BPNSs-TPA}$ -based resistive switching memory.

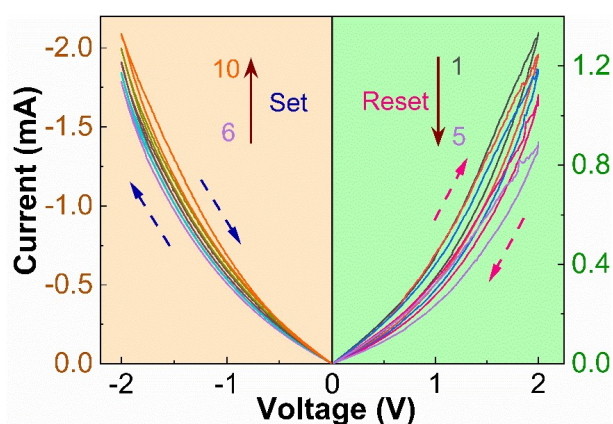


Figure S10. a) Potentiation and b) depression processes of the $\text{EV}(\text{ClO}_4)_2/\text{BPNSs-TPA}$ -based resistive switching memory. The amplitude, duration, and period of the voltage pulses are ± 2 V, 10 ms, and 2 s, respectively.

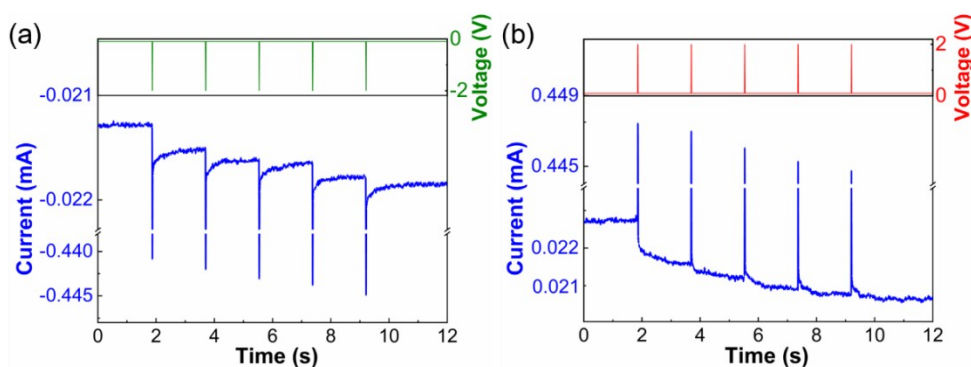
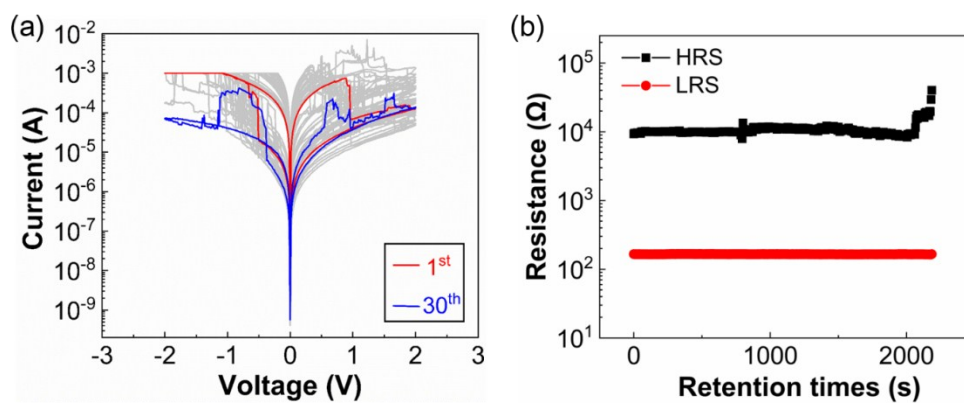


Figure S11. Control experiment analysis. a) I - V characteristics for and b) Retention ability of $\text{EV}(\text{ClO}_4)_2/\text{BPNSs}$ device.



References

1. F. L. Floch, J.-P. Simonato, G. Bidan, *Electrochim. Acta*, 2009, **54**, 3078-3085.
2. R. Kumar, R. G. Pillai, N. Pekas, Y. Wu, R. L. McCreery, *J. Am. Chem. Soc.*, 2012, **134**, 14869-14876.